

# EVALUATION OF HYDRAULIC PROPERTIES OF THE ARTIFICIAL SUBSURFACE SYSTEM IN HIGASHIHACHIMANTAI GEOTHERMAL MODEL FIELD

HAYASHI, K., Institute of High Speed Mechanics, Tohoku Univ., Sendai 980, Japan  
ABÉ, H., Dept. of Mechanical Eng., Tohoku Univ., Sendai 980, Japan

## 1. INTRODUCTION

In the  $\Gamma$ -Project, Tohoku University, a subsurface system, which consists of an artificial, globally flat crack and two wells, were successfully constructed as designed (Takahashi and Abé, 1988). After the connection of the two wells through the reservoir crack, experiments to examine the hydraulic properties of the subsurface system were performed. The experiments were the transmissivity tests, the circulation tests and the tracer test.

The objective of the present paper is two fold. The first is to evaluate the hydraulic properties of the subsurface system of the  $\Gamma$ -Project and the second is to develop the methods to predict the flow impedance and to estimate the area of the effective heat exchange surface from the tracer tests. To this end, the water pressure and velocity distribution of the flow in a penny shaped crack with an inlet and an outlet are analyzed, where the water loss during the circulation is appropriately taken into account. The transmissivity can be obtained by the straight forward manner proposed by Jung (1987). Based on the analysis just stated, the flow impedance can be expressed as a function of the crack size, the transmissivity and the location of the inlet and the outlet. Therefore, the flow impedance is predictable when these are given. This approach is applied to the subsurface system of the  $\Gamma$ -Project. The application results show that the approach gives excellent predictions. As to the evaluation of the area of effective heat exchange surface, the time variation of the tracer concentration at the outlet during the tracer test is firstly simulated based on the analysis of the flow stated before. The outlet tracer return profile so constructed is compared with the results of the tracer test to evaluate the area of the effective heat exchange surface. It has been found that the area is approximately 470 m<sup>2</sup>.

## 2. ANALYSIS OF FLOW IN A PENNY SHAPED CRACK WITH AN INLET AND OUTLET

Let us consider a penny shaped crack with an inlet and an outlet, where the penny shaped crack is a model of the propped region of an artificially created flat crack. The propped region is expected to have low enough flow resistance compared with the unpropped region and the most amount of the injected water is assumed to flow in the propped region. Here, the water flowing out to the unpropped region is assumed not to return to the outlet and is treated as water loss. Let us introduce a Cartesian coordinate system (x, y) centered at the center of the penny shaped crack as in Fig. 1, where a is the crack radius and r<sub>i</sub> and r<sub>o</sub> are the radii of the inlet and outlet wells. Throughout this paper, the lower indices i and o stand for the inlet (or the injection well) and the outlet (or the production well) unless otherwise stated. The inlet and outlet positions are (x, y) = (-l, 0) and (l, 0), respectively. The aperture b and the transmissivity T are assumed to be constant throughout the crack.

The equation of continuity and the equation of motion (Jung, 1987) are

$$\frac{\partial q_x}{\partial x} + \frac{\partial q_y}{\partial y} = 0 \quad (1)$$

$$q_x = -\frac{T}{\mu} \frac{\partial p}{\partial x}, \quad q_y = -\frac{T}{\mu} \frac{\partial p}{\partial y} \quad (2)$$

where q<sub>x</sub> (or q<sub>y</sub>) is the volumetric flow rate of the water flowing in the x(or y)-direction across the unit length in the y(or x)-direction,  $\mu$  the water viscosity and p the water pressure. From eqs. (1) and (2), it is readily understood that p is a plane harmonic function and, therefore, a complex function w(z) (z = x + iy, i: pure imaginary), which is holomorphic in the region |z| < 1 except for the points (±l, 0), can be introduced as w(z) = p(x, y) + iψ(x, y) with ψ(x, y) being the conjugate harmonic function of p(x, y). It is readily seen from the Cauchy-Riemann relation and eq. (2) that the lines ψ(x, y) = const. are the stream lines. Equation (2) leads to

$$q_x = -\frac{T}{\mu} \operatorname{Re}(dw/dz), \quad q_y = \frac{T}{\mu} \operatorname{Im}(dw/dz) \quad (3)$$

where Re(·) and Im(·) represent the real and imaginary parts, respectively.

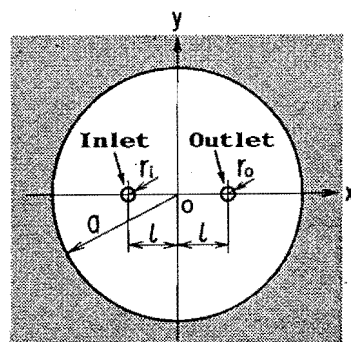


Fig. 1. Penny shaped crack and coordinate system.

Let us set the logarithmic singularities at the points  $(-l, 0)$ ,  $(l, 0)$ ,  $(-a^2/l, 0)$  and  $(a^2/l, 0)$  with the intensities  $w_0$ ,  $-aw_0$ ,  $w_0$  and  $-aw_0$ , where  $\alpha$  ( $< 1$ ) is the rate of the water recovery and

$$w_0 = \frac{\mu Q_i}{2\pi T} \quad (4)$$

with  $Q_i$  being the inlet volumetric flow rate. Let us also distribute continuously the logarithmic singularities with the intensity  $(1-\alpha)w_0/(\pi a)$  per unit length along  $|z| = a$ . Then, we have

$$w(z) = w_0 \left[ \ln \frac{z+l}{z+a^2/l} - \ln \frac{z}{l} \right] - \alpha \left[ \ln \frac{z-l}{z-a^2/l} - \ln \frac{z}{l} \right] + (1-\alpha) \ln \frac{z}{l} \quad (5)$$

The pressure distribution of the flow expressed by  $w(z)$  given by eq. (5) is

$$p(x, y) = \text{Re}\{w(z)\} = w_0 \ln \frac{r_2 r_4}{r_1 \alpha r_2 \alpha^2 (1-\alpha)} \quad (6)$$

where  $r_1, \dots, r_4$  are the distances to  $(x, y)$  from the points  $(l, 0)$ ,  $(-l, 0)$ ,  $(a^2/l, 0)$  and  $(-a^2/l, 0)$ , respectively. It should be noted that the pressure given by (6) represent the pressure difference between the point  $(x, y)$  and the origin.

### 3. TRANSMISSIVITY AND FLOW IMPEDANCE

#### 3.1. Field Experiment and Experimental Results

The subsurface system of the  $\Gamma$ -Project consists of a flat artificial crack and two wells, F-1 and EE-4. The crack strikes N60°E and dips N47°, and the wells F-1 and EE-4 are crossing the crack at 366 m and 357 m depths, respectively. For the transmissivity experiment, the well F-1 was closed and the water injected from the well EE-4 at constant volumetric flow rates. The flow rates used were 5.6, 9.1, 16.9, 24, 30 and 40 l/min. The pressures of the both wells and the pressure difference between them were monitored. Figure 2 shows a typical example of the time variation of the pressures, where  $p_o$  and  $p_i$  are the downhole pressures of the observation (F-1) and injection (EE-4) wells, respectively. As shown in Fig. 2, the pressures increased in the first stage of the injection and finally leveled off. The transmissivity is evaluated by the following equation (Jung, 1987):

$$T = \frac{\mu Q_i}{2\pi \Delta p} \ln \frac{2l}{r_i} \quad (7)$$

with  $\Delta p$  being the downhole pressure difference after the pressures leveled off (Fig. 2). Figure 3 shows the transmissivity. Here,  $r_i = 5$  cm,  $l = 3.5$  m and  $\mu = 4 \times 10^{-9}$  kg.sec/cm<sup>2</sup> have been used. The solid line is the line obtained by the least-square method. The pressure  $p_{or}$  in Fig. 3 is the downhole pressure of the observation well after it leveled off (Fig. 2). This pressure is considered to represent approximately the average pressure in the crack, since the pressure gradient is very small in the crack except for the very vicinity of the injection well (Jung, 1987).

After the transmissivity experiment, two series of circulation experiments, i.e., the circulations from EE-4 to F-1 and from F-1 to EE-4, were performed at various volumetric flow rates. The production well was open at the surface, and the surface pressure of the injection well and the volumetric flow rate from the production well were monitored. The flow impedance  $I$  is determined by

$$I = \frac{\Delta P}{Q_i} \quad (8)$$

where  $\Delta P$  is the surface pressure difference between the two wells after the pressure of the injection well leveled off. The results are shown in Fig. 4. As to the solid lines in Fig. 4, see the following subsection.

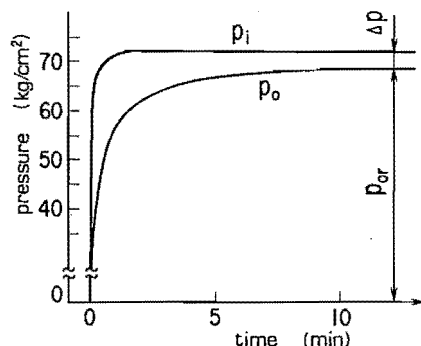


Fig. 2. Pressure records during the transmissivity experiment ( $Q_i = 30$  l/min).

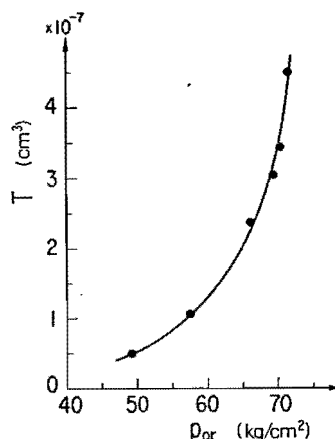


Fig. 3. Transmissivity against the reservoir pressure.

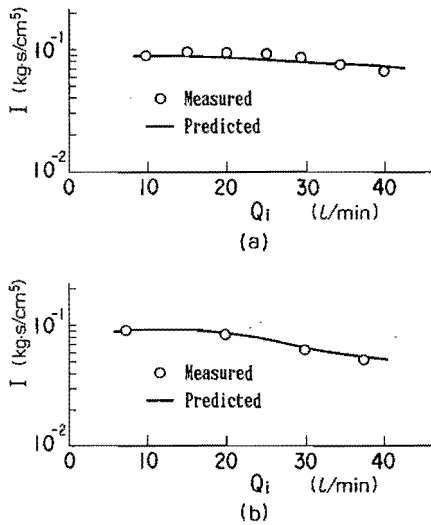


Fig. 4. Flow impedance against inlet flow rate. (a) circulation from EE-4 to F-1, (b) circulation from F-1 to EE-4.

Numbers of the flow in the wells. In the case of the subsurface system of the  $\Gamma$ -Project,  $\Delta p_h$  and  $\Delta p_f$  are negligibly small. The solid lines in Fig. 4 are indicating the predictions, where  $\ell$  and  $a$  is set to be 3.5 m and 40 m, respectively, and  $\alpha$  is chosen to be 0.74 following the experimental results. Since the crack size cannot necessarily be specified definitely, the calculations for other crack sizes ranging from 30 m to 60 m were also performed. However, the predictions were nearly the same.

#### 4. TRACER EXPERIMENT AND EFFECTIVE AREA OF HEAT EXCHANGE SURFACE

##### 4.1. Tracer Experiment and Experimental Results

The tracer experiment involved placement of 300 l of 28700 ppm aqueous solution of NaCl. The tracer, then, pumped down at 30 l/min through F-1, the reservoir crack and EE-4 back to the earth's surface. The electric resistivity of the water was monitored at the depth, where EE-4 is crossing the crack, to obtain the time variation of the tracer concentration at the outlet of the crack. The first arrival was observed after about 4 hr after the injection of the tracer started. The rate of water recovery  $\alpha$  was 0.8 during the tracer experiment. Figure 5 shows the outlet tracer response obtained by the experiment, where  $c$  is the concentration at the outlet of the crack,  $c_0$  the initial concentration at the wellhead of F-1 and  $t$  time.

##### 4.2. Area of Effective Heat Exchange Surface

Usually, the informations drawn from tracer experiments are those on volumes of reservoirs such as modal volumes and integral mean volumes (Tester et al., 1982; Robinson and Tester, 1984). Here, in this subsection, the area of the surface which was swept by the recovered water is examined. The stream line flow dispersion is considered. The dispersion in the transverse direction (Horne and Rodriguez, 1983) is not taken into account following Robinson and Tester (1984).

As stated in the Section 2, the lines  $\psi(x, y) = \text{const.}$  are the stream lines. Figure 6 shows the stream lines in the upper half of the crack schematically. It is easily seen from eq. (5) that the water flowing out from the inlet in a direction making an angle with the x-axis larger than  $\alpha\pi$  never returns to the outlet (Fig. 6). The resident time along a stream line (say  $\Gamma$  (Fig. 6)) is given by

##### 3.2. Prediction of Flow Impedance

Let  $p^f$  and  $h$  be the pressure loss caused in the well and the depth where the well is crossing the crack. Then, the flow impedance can be expressed as follows:

$$I = \frac{(p_i - p_o) - \Delta p_h + \Delta p_f}{Q_i} \quad (9)$$

$$\Delta p_h = \rho g(h_i - h_o), \quad \Delta p_f = p_i^f + p_o^f$$

where  $\rho$  is the water density and  $g$  the acceleration due to gravity. The pressures  $p_i$  and  $p_o$  are the downhole pressures of the injection and production wells, respectively. With the aid of eqs. (4) and (6), eq. (9) becomes

$$I = \frac{\mu}{2\pi T} (p_{in} - p_{on}) + \frac{1}{Q_i} (-\Delta p_h + \Delta p_f) \quad (10)$$

$$p_{in} = \ln \frac{r_i(a^2/\ell - \ell + r_i)}{(2\ell - r_i)^\alpha (a^2/\ell + \ell - r_i)^\alpha a^{2(1-\alpha)}} \quad (11)$$

$$p_{on} = \ln \frac{(2\ell - r_o)(a^2/\ell + \ell - r_o)}{r_o^\alpha (a^2/\ell - \ell + r_o)^\alpha a^{2(1-\alpha)}} \quad (12)$$

Therefore, if  $r_i$ ,  $r_o$ ,  $a$ ,  $\alpha$ ,  $\ell$ ,  $T$  and  $\Delta p_h$  are given, the flow impedance can be predicted by eqs. (10)-(12), where  $\Delta p_f$  can be estimated for given Reynolds

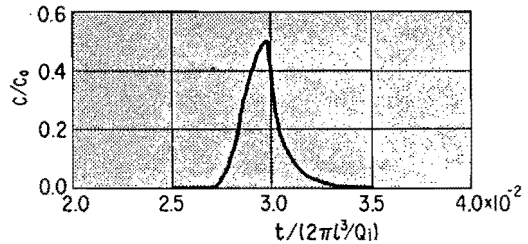


Fig. 5. Outlet tracer response obtained from the tracer experiment.

$$T(\theta) = \int_{\Gamma} \frac{b \, ds}{(q_x^2 + q_y^2)^{1/2}} \quad (13)$$

where  $q_x$  and  $q_y$  are given by eqs. (3) and (5) and  $\theta$  is the angle between the stream line and the x-axis at the inlet (Fig. 6). Let  $c_{in}(t)$  be the tracer concentration at the inlet. Then, the mass of the tracer reaching the outlet during  $t \sim t + \Delta t$  along  $\Gamma$  is given by  $(\rho Q_i / (2\pi)) c_{in}(t - T(\theta)) \Delta t$  and the mass of water reaching the outlet during  $t \sim t + \Delta t$  is  $\rho \alpha Q_i \Delta t$ . Therefore, the outlet tracer response  $c(t)$  is given by

$$c(t) = \frac{1}{2\pi\alpha} \int_{-\alpha\pi}^{\alpha\pi} c_{in}(t - T(\theta)) d\theta \quad (14)$$

In the tracer experiment of the  $\Gamma$ -Project, the tracer injected at the wellhead of F-1 as stated before and, as a result,  $c_{in}(t)$  is not known. Here,  $c_{in}(t)$  is estimated based on the convective dispersion of the flow in a pipe, where the radial distribution of the axial velocity  $u(r)$  in the pipe is assumed to be  $u(r) = u_0(1-r/r_i)^\lambda$  as usually used. As can be recognized,  $c(t)/c_0$  is dependent on the crack radius  $a$ , the aperture  $b$  and the exponent  $\lambda$ . These parameters are determined so as to make the maximum height, the width at 1/2 height and the width of 1/4 height of the simulated outlet tracer response be equal to those of the experimental outlet tracer response (Fig. 5). The results are  $a = 35$  m,  $b = 0.9$  mm and  $\lambda = 0.021$ . The simulated outlet tracer response for these values of the parameters is shown in Fig. 7, and the stream lines which provide this outlet tracer response are shown in Fig. 8 for the upper half of the crack. The hatched region in Fig. 8 is the surface which is swept by the water recovered through the outlet, i.e., the effective heat exchange surface. The area of this region is  $470 \text{ m}^2$  approximately. Although the cases with different inlet and outlet positions were also simulated, the outlet tracer responses were almost the same except for the cases that the inlet and outlet were in the vicinity of the crack periphery.

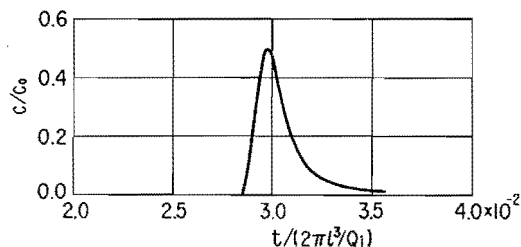


Fig. 7. Outlet tracer response obtained by the simulation.

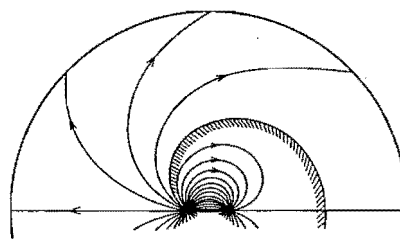


Fig. 8. Stream lines corresponding to Fig. 6. Recovered water sweeps the hatched region.

## REFERENCES

- Horne, R. N. and Rodríguez, F. (1983) Dispersion in Tracer Flow in Fractured Geothermal Systems, *Geophys. Res. Lett.*, 10, 289-292.
- Jung, R. (1987) Hydraulic In-Situ Investigations on an Artificial Fracture in the Falkenberg Granite, presented at the Workshop on Forced Fluid Flow through Strong Fractured Rock Masses, Garchy, France, Aripil 12-15.
- Robinson, B. A. and Tester, J. W. (1984) Dispersed Fluid Flow in Fractured Reservoirs: An Analysis of Tracer - Determined Resistance Time Distributions, *J. Geophys. Res.*, 89, 10374-10384.
- Tester, J. W., Bivins, R. L. and Potter, R. M. (1982) Interwell Tracer Analysis of a Hydraulically Fractured Granitic Geothermal Reservoir, *Soc. Pet. Engng. J.*, 22, 537-554.
- Takahashi, H. and Abé, H. (1988) Design Methodology of Artificial Crack-Like Reservoirs for HDR Geothermal Energy Extraction - An Overview of the  $\Gamma$ -Project in Japan, *Geothermal Energy Symposium, ASME*, 25-32.